# Flocculation of Biological Cells: Experiment vs. Theory

**Binbing Han, S. Akeprathumchai, and S. R. Wickramasinghe**
Dept. of Chemical Engineering

**X. Qian**
Dept. of Physics

Colorado State University, Fort Collins, CO 80523

*Flocculation of biological cells is important in the biotechnology industry, as it could lead to improved efficiencies for bioreactor harvesting operations such as microfiltration. Experimental studies for flocculation of yeast and CHO cells using cationic polyelectrolytes suggest the existence of a steady-state, self-similar floc size distribution. The experimentally determined floc size distributions were modeled using a population balance approach. For flocculated yeast suspensions, the variation of the floc volume fraction with dimensionless particle diameter is predicted by the population balance model assuming a binary breakage distribution function. However, the variation of floc number fraction with dimensionless particle diameter is better predicted assuming a log normal fragment distribution function probably due to the presence of submicron-sized yeast cell debris. For CHO cell flocs, the floc volume and number fractions are predicted using a log normal fragment distribution function. CHO cells are far more fragile than yeast cells. Thus, individual CHO cells in a CHO cell floc can lyse leading to the formation of a number of small particles.*

## Introduction

Flocculation of particles is important in a number of fields such as biotechnology, colloidal and polymer science, and astronomy (Shamlou and Tichener-Hooker, 1993; Friedlander, 1977; Silk, 1980). Flocculation of fine particulate matter is an important pretreatment step in the liquid-solid separation process in a number of industrial applications (Blatz and Tobolsky, 1954; Coulaloglou and Tavlarides, 1977; Danov et al., 1994). The first of the purification operations in the manufacture of biotechnological products usually involves the separation of cells and cell debris from the suspending medium. Frequently, the desired product is excreted by the cells into the suspending medium. Microfiltration is often used to separate the suspending medium from the cells and other insoluble particulate matter. In this work we focus on flocculation of cell suspensions in order to improve the efficiency of unit operations such as microfiltration which are used in the biotechnology industry.

Correspondence concerning this article should be addressed to S. R. Wickramasinghe.

Biological feeds are notoriously difficult to filter either, because they are highly non-Newtonian, or because the cake formed is highly fouling (Belter et al., 1988). During filtration, these cakes deform into an impermeable mat resulting in very low permeate fluxes and high-pressure drops. The filterability of the feed may also depend on the cell viability at the time of bioreactor harvesting. A low cell viability means a large number of the cells present are dead. These dead cells lyse, producing smaller particles that can easily plug the membrane pores. One way to improve the filterability of biological feeds is to treat them prior to microfiltration. Previous investigators (Aunins and Wang, 1989; Gasner and Wang, 1970; Baran, 1988; Hughes et al., 1990; Kim et al., 2001) have shown that addition of synthetic polymeric flocculants to cell suspensions leads to an increase in the average particle size. Since the permeate flux during microfiltration increases with particle size (Belfort et al., 1994), increasing the particle size by flocculation should lead to higher permeate fluxes.

Flocculation of cell suspensions will lead to a distribution of particle sizes. A number of investigators (Kim et al., 2001; Dharmappa et al., 1992; Wickramasinghe, 1999; Huisman et

al., 1999; Tanaka et al., 1994; Chellam and Wiesner, 1998) have shown that, for polydisperse feeds, the presence of smaller particles often leads to lower permeate fluxes during microfiltration than would be expected based on the average particle size. Thus, determining the properties of the particle-size distribution after flocculation is essential in order to predict the effect of flocculation on the permeate flux.

In biotechnology applications, the flocculant is added to the bioreactor in order to destabilize the suspension. Previous investigators have reported studies using positively, neutrally, and negatively charged flocculants (Aunins and Wang, 1989; Gasner and Wang, 1970; Baran, 1988; Hughes et al., 1990; Kim et al., 2001). In general positively charged flocculants are the most successful since the cells are negatively charged. For flocculation to occur, collisions are essential between particles. Thus, after addition of the polymer, the suspension is stirred in order to ensure thorough mixing and, hence, a high collision frequency. Initially, the flocs grow rapidly. However, as the flocs become larger, they can be fragmented by fluid particle interactions. Consequently, in this work we focus on simultaneous shear induced flocculation and fragmentation.

A population balance equation may be used to model the floc size distribution (Ramkrishna, 2000). The population balance equation accounts for various ways in which particles of a specific state can either form or disappear from the system. A common approach has been to combine the collision frequency for shear induced flocculation with a mathematical expression for particle fragmentation.

Since the rates of flocculation and fragmentation depend on the size of the floc, a steady-state floc size distribution can arise favoring floc sizes in the range in which the time scales of the two processes balance each other. The existence of a steady-state floc size distribution has been shown experimentally by a number of investigators. For example, steady-state floc size distributions have been observed for monodisperse polystyrene particles in distilled water (Spicer and Pratsinis, 1996), kaolinite clay suspension (Tambo and Watanabe, 1979; Lu and Spielman, 1985) and for dispersed phase droplets in a liquid-liquid dispersion (Zeitlin and Tavlarides, 1972). Reich and Vold (1959) found that a steady floc size distribution existed for flocculation of aqueous suspensions of carbon and ferric hydroxide in water.

Vigil and Ziff (1989) have investigated numerically the existence of a steady-state floc size distribution. They determined conditions under which a steady-state distribution exists for different functional forms of the flocculation and fragmentation rates. If the dimensionless steady-state floc size distributions obtained under different conditions can be collapsed onto the same curve, the distribution is said to be self-similar. Ramkrishna (2000) has discussed in detail the existence of a self-similar floc size distribution. Obtaining such a distribution is of considerable value not only in the characterization of experimental data, but also in order to identify key model parameters associated with the system behavior.

Most prior experimental and theoretical studies have focused on flocculation of inorganic feed streams. This article focuses on flocculation of feedstreams of significance to the biotechnology industry. In particular, experiments have been conducted using both yeast and CHO cells. Yeast cells were chosen since they have been used in previous microfiltration studies (Kim et al., 2001; Bell and Davies, 1987; Ofsthun, 1989; Patel et al., 1987; Russotti et al., 1995). In addition yeast cells make a good model system, as they are nondeformable rigid spheroids with a major radius of about 3.5 $\mu$m and a minor radius of 2.7 $\mu$m. CHO cells are frequently used in the biotechnology industry. The yeast and CHO cell feedstreams were flocculated using commercially available cationic polymeric flocculants obtained from Cytec Industries (Stamford, CT). The steady-state floc size distributions determined experimentally are compared to the predictions based on the population balance model.

## Theory

The rate of change with time of the volume fraction of particles of size $i$ is given by

$$\frac{d\nu_i}{dt} = \frac{1}{2}\sum_{j+k=i}\alpha_{jk}\beta_{jk}\nu_j\nu_k - \nu_i\sum_{k=1}^{\max}\alpha_{ik}\beta_{ik}\nu_k - S_i\nu_i + \sum_{j=i+1}^{\max}\gamma_{ij}S_j\nu_j \quad (1)$$

where $\nu_i$, $\nu_j$, and $\nu_k$ are the volume fraction of particles of size $i$, $j$, and $k$; $\alpha_{jk}$ is the collision efficiency between two colliding particles $j$ and $k$; $\beta_{jk}$ is the collision frequency between two particles $j$ and $k$; $S_i$ is the fragmentation rate of particles of size $i$; and $\gamma_{ij}$ is the fragment distribution function of size $i$ coming from $j$-sized particles.

It is assumed that the density of the floc particles is constant; consequently, the total volume of particulate matter present is constant throughout the flocculation process. Thus, $\nu_i$ is the volume of all particles of size $i$ divided by the total volume of particulate matter present. The first and fourth terms on the righthand side in Eq. 1 represent rates of production of particles of size $i$, while the second and third terms represent the destruction of flocs of size $i$.

The first two terms are flocculation terms. The first term gives the rate of formation of flocs of size $i$ due to collisions between two smaller particles of size $j$ and $k$. In this expression $\alpha_{jk}$, the collision efficiency, gives the fraction of collisions that lead to flocculation and $\beta_{jk}$ gives the frequency of collisions between particles $j$ and $k$. The summation in the first term is for all combinations of particles that will produce a new particle of size $i$. Since collisions between particles of $j$ and $k$ are the same as between particles of $k$ and $j$, the factor 1/2 is added. As can be seen, the first term depends on the volume fraction $\nu_j$ and $\nu_k$ of the colliding particles. The second term gives the rate of disappearance of particles of size $i$ due to collision with other particles.

The third and fourth terms are fragmentation terms. The third term gives the rate of fragmentation of particles of size $i$ where $S_i$ is the fragmentation rate. The fourth term gives the rate of production of particles of size $i$ due to fragmentation of larger particles of size $j$. $\gamma_{ij}$ is the fragment distribution function. Equation 1 may also be expressed in terms of

**Table 1. Literature Expressions for the Collision Efficiency**

| No. | Expression | Ref. | Comments |
|---|---|---|---|
| 1 | $\alpha_{ij} = \dfrac{\pi\left(s\sin\theta^* \dfrac{d_i + d_j}{4}\right)^2 \left(as\cos\theta^* \dfrac{d_i + d_j}{2}\right)}{0.29(d_i + d_j)^3 G}$ | Chin et al. (1998) | Flocculation of polystyrene and magnetite particles |
| 2 | $\alpha_{ij} = \alpha_o \left(1 - \dfrac{d_i + d_j}{2d_{\max}}\right)^c$ | Koh et al. (1987) | Flocculation of scheelite sodium oleate system |
| 3 | $\alpha_{ij} = 1$ | Spicer et al. (1996a); Saffman and Turner (1956); Spicer and Pratsinis (1996) | Assumes all collision will lead to flocculation |

the number fraction of particles of size $i$.

$$\frac{dn_i}{dt} = \frac{1}{2}\sum_{j+k=i} \alpha'_{jk}\,\beta'_{jk} n_j n_k - n_i \sum_{k=1}^{\max} \alpha'_{ik}\,\beta'_{ik} n_k - S'_i n_i + \sum_{j=i+1}^{\max} \gamma'_{ij} S'_j n_j \quad (2)$$

where $n_i$ is the number concentration of flocs of size $i$ divided by the total number of particle present. $\alpha'_{jk}$, $\beta'_{jk}$, $S'_i$, and $\gamma'_{ij}$ are still the collision efficiency between two colliding particles $j$ and $k$, the collision frequency between two particles $j$ and $k$, the fragmentation rate of particles of size $i$, and the fragment distribution function of size $i$ coming from $j$-sized particles. However, the total number of particles present is not constant, but is a function of time for a given set of experimental conditions.

Equations 1 and 2 may be solved once appropriate expressions have been found for the parameters $\alpha_{jk}$, $\beta_{jk}$, $S_i$, and $\gamma_{ij}$ or $\alpha'_{jk}$, $\beta'_{jk}$, $S'_i$ and $\gamma'_{ij}$. Each of these parameters is discussed below.

### *Collision efficiency*

In this work it is assumed that the population density is small such that during a time interval $dt$, the probability of more than two particles aggregating simultaneously to form a single particle is only of order $O(dt^2)$, while that of two particles aggregating is of order $O(dt)$. Thus we consider only two body interactions, as have many previous investigators (Batterham et al., 1981; Koh et al., 1987; Hounslow et al., 1988; Berlin et al., 1997; Kislenko, 2000; Spicer and Pratsinis, 1996; Spicer et al., 1996a). McAnally and Mehta (2000) have developed a collision efficiency factor for three body interaction. However, even for particle volume fractions of 10%, the ratio of three body to two body interaction is only 0.05.

Collision efficiencies used in several past studies are summarized in Table 1. Some previous investigators have derived specific functional forms for the collision efficiency. Chin et al. (1998) studied the flocculation of polystyrene and magnetite particles. They developed a model by using trajectory analysis and a population balance equation. They determined their collision efficiency by taking the ratio of the flocculation rate when interparticle forces and hydrodynamic mobility are taken into account to the flocculation rate in the absence of these factors. However, the collision efficiency that they predict assumes the Saffman and Turner (1956) equation for the collision frequency (see below). Koh et al. (1987) derived an empirical expression for the flocculation efficiency. This equation gave satisfactory results for the flocculation of a scheelite-sodium oleate system.

Numerous past investigators have assumed a collision efficiency of 1 (Spicer et al., 1996a; Saffman and Turner, 1956; Spicer and Pratsinis, 1996). This implies that, if two particles were to collide, they will stick together. Since biological cells often aggregate naturally, in this work it will be assumed that the collision efficiency is 1.

**Table 2. Literature Expressions for the Collision Frequency**

| No. | Expression | Ref. | Comments |
|---|---|---|---|
| 1 | $\beta_{ij} = \dfrac{2kT}{\mu}(d_i + d_j)\left(\dfrac{1}{d_i} + \dfrac{1}{d_j}\right)$ | Smoluchowski (1916) | Perkinetic flocculation |
| 2 | $\beta_{ij} = \dfrac{1}{6} G (d_i + d_j)^3$ | Smoluchowski (1917); Camp and Stein (1943); Koh et al. (1987) | Orthokinetic flocculation |
| 3 | $\beta_{ij} = \dfrac{2.3}{8} G (d_i + d_j)^3$ | Chin et al. (1998); Saffman and Turner (1956); Spicer and Pratsinis (1996); Spicer et al. (1996a) | Turbulent flow |
| 4 | $\beta_{ij} = \dfrac{\pi}{4} F_c^2 \sqrt{\dfrac{2}{15\pi}}\, G (d_i + d_j)^3$ | McAnally and Mehta (2000) | Aggregation of estuarial fine sediment |
| 5 | $\beta_{ij} = 1.25(d_i + d_j)^2 \sqrt{\dfrac{\overline{U}^2}{1 + 1.5\tau_1 \epsilon/\overline{U}^2} + \dfrac{\overline{U}^2}{1 + 1.5\tau_2 \epsilon/\overline{U}^2}}$ | Abrahamson (1975) | Turbulent flow |

### *Collision frequency*

Collision frequencies used in some past studies are summarized in Table 2. The collision frequency depends upon the prevailing hydrodynamic conditions. Perikinetic flocculation occurs in a quiescent system where collisions between particles occur due to their Brownian motion. Smoluchowski (1916) determined the collision frequency for perikinetic flocculation. Since perikinetic flocculation is slow for particles 1 $\mu$m or larger in diameter, it is not expected to be significant for the flocculaton of cells.

Orthokinetic flocculation occurs in a laminar shear field. Flocculation under these conditions is useful in experimental studies since the flow field is well defined. Smoluchowski (1917) also determined the collision frequency for orthokinetic flocculation. However, most practical flocculators are operated in a stirred tank under turbulent conditions, thus ensuring thorough mixing and hence a high collision frequency between particles and, therefore, rapid floc growth.

Saffman and Turner (1956) derived an expression for the collision frequency of small drops in turbulent flow. Two major assumptions in their equation are that the drops are approximately equal in size and that the drops are much smaller than the smallest turbulent eddies present. Consequently, the collision rate depends only on the dimensions of the drops, the rate of energy dissipation and the kinematic viscosity of the fluid. In their original article Saffman and Turner (1956) give the numerical constant as 1.3, rather than 2.3 (see Table 2, Eq. 3). Although this error was corrected by Pearson et al. (1984), the original incorrect form of the equation has been used (Spicer and Pratsinis, 1996; Spicer et al., 1996a). Saffman and Turner (1956) also determined the collision frequency for drops with different inertia due to gravity and turbulent accelerations. McAnally and Mehta (2000) provide an equation for the collision frequency that is very similar to that of Saffman and Turner for the aggregation of estuarine sediment.

Biological feed solutions do not consist of equal sized particles. As well as cells, cell debris and other insoluable submicron sized particulate matter is present (Kim et al., 2001). Further, as the floc particles start to grow, it is unlikely that they will be much smaller than the smallest turbulent eddies present. Nevertheless, several previous investigators have used the Saffman and Turner equation for flocculation of inorganic systems such as polystyrene particles (Spicer and Pratsinis, 1996) and polystyrene and magnetite particles (Chin et al., 1998) where it is unlikely that the two major assump-

**Table 3. Literature Expressions for Fragment Distribution Functions Which Allow a Self-Similar Solution**

| No. | Expression | Ref. | Comments |
|---|---|---|---|
| 1 | $\gamma_{ij} = cu_j/u_i$ | Spicer et al. (1996a); Spicer and Pratsinis (1996) | For binary fragment, $c = 1$, $j = i+1$; for ternary fragment, $c = 2$, $j = i$, $i+1$; and for quaternary fragment, $c = 1$, $j = i+2$ |
| 2 | $\gamma_{ij} = \frac{u_j}{u_i}\int_{b_{i-1}}^{b_i} \frac{1}{\sqrt{2\pi}\log\sigma}\exp\left[-\left(\frac{\log(u/u_m)}{\log\sigma}\right)^2\right]du$ | Pandya and Spielman (1982); Lu and Spielman (1985) | Log normal distribution as defined by Mochizuki and Zydney (1993) |
| 3 | $\gamma_{ij} = \frac{u_j}{u_i}\int_{b_{i-1}}^{b_i} \frac{1}{\sqrt{2\pi}\sigma}\exp\left[-\frac{(u-u_m)^2}{2\sigma^2}\right]du$ | Spicer and Pratsinis (1996) | Normal distribution |
| 4 | $\gamma_{ij} = B(u_i,u_j) - B(u_{i-1},u_j)$ | Kusters et al. (1993) | Ultrasonic fragmentation |
| 5 | $\gamma_{ij} = \frac{(u_i/u_j)^{-5/3}\exp\left(-(u_i/u_j)^{1/3}\right)}{3u_j(1-1/e)}$ | Broadbent and Calcott (1956) | Milling |
| 6 | $\gamma_{ij} = \frac{r(u_i/u_j)^{-5/3}\left(1-(u_i/u_j)^{1/3}\right)^{r-1}}{3u_j}$ | Gaudiin and Meloy (1962) | Random fracture |
| 7 | $\gamma_{ij} = \frac{ac(u_i/u_j)^{c-2}+(1-a)d(u_i/u_j)^{d-2}}{u_j}$ | Shoji et al. (1980) | Milling |
| 8 | $\gamma_{ij} = \frac{1}{3u_j(u_i/u_j)^{5/3}}$ | Reid (1965) | Theoretical |
| 9 | $\gamma_{ij} = \frac{n(u_i/u_j)^{n-2}}{u_j}$ | Randolph and Ranjan (1977) | Theoretical |
| 10 | $\gamma_{ij} = \frac{2\exp\left[-(u_i-u_j/2)^2/2\sigma^2\right]}{\sqrt{2\pi}\sigma\left[\mathrm{erf}\left(\frac{u_j}{2\sqrt{2}\sigma}\right)\right]}$ | Gelbard and Peterson (1983); Pandya and Spielman (1982) | Theoretical |
| 11 | $\gamma_{ij} = \frac{2(2n+1)(2u_i/u_j-1)^{2n}}{u_j}$ | Gelbard and Peterson (1983) | Fly ash formation |
| 12 | $\gamma_{ij} = \frac{K(\sigma,cu_j)\exp[-\ln^2(u_i/cu_j)/2\ln^2\sigma]}{u_i}$ | Peterson (1984) | Fly ash formation |

tions of the Saffman and Turner equation are valid. Therefore, the Saffman and Turner equation (Saffman and Turner, 1956) will be used in this work.

Abrahamson (1975) also considered flocculation in turbulent systems in the absence of body forces such as gravitational and centrifugal forces. However, he considered the case where larger particles exist or more vigorous fluid turbulence meant that the fluid and particle velocities may not coincide. In this study it is likely that as the floc particles start to grow, the fluid and particle velocities will not coincide. Thus, the equation derived by Abrahamson will also be used in this work. We shall compare the results obtained using the Saffman and Turner equation (Saffman and Turner, 1956) and the Abrahamson equation (Abrahamson, 1975).

### *Fragmentation rate*

In grinding applications such as ball mills, it is often found that the fragmentation rate is given by the equation

$$S_i = A\left(\frac{u_i}{u_{\max}}\right)^{\delta} \tag{3}$$

where $A$ is the specific fragmentation rate for the largest particles present, $\delta$ is a constant, $u_i$ is the volume of particle $i$, and $u_{\max}$ is the volume of the largest particle present (Ray and Hogg, 1987; Peng and Williams, 1994). For the fragmentation of flocs, Eq. 3 is often written in the form (Pandya and Spielman, 1982)

$$S_i = A' G^{\delta'} u_i^{\delta''} \tag{4}$$

Assuming that the floc fragmentation rate is proportional to floc diameter (Boadway, 1978; Peng and Williams, 1994), $\delta''$ is 1/3. Pandya and Spielman (1982) and Spicer and Pratsinis (1996) found $\delta'$ to be 1.6 for kaolin and polystyrene flocs, respectively. Oles (1992) found $A'$ to be 0.0047. These values will be used in this work. Kapur (1972) and Ramkrishna (2000) have shown that this type of power law fragmentation will permit a self-similar solution for fragmentation processes.

### *Fragment distribution function*

Numerous fragment distribution functions have been described in the literature, some of which are summarized in Table 3. Four fragment distribution functions will be considered: binary fragmentation, where the two fragments produced are of approximately equal volume; ternary fragmentation, where three fragments are produced, two of which have the same volume while the third fragment is larger; quaternary fragmentation, where four fragments of approximately equal volume are produced; and log normal fragmentation, where the fragments produced are distributed according to the log normal distribution.

Binary fragmentation is the simplest. It is likely that when relatively small yeast flocs fragment two approximately equally sized particles are formed. Larger yeast flocs could fragment into three or four particles, as described by the ternary and quaternary fragment distribution functions. However, it is unlikely that the individual yeast cells will lyse during the flocculation process.

CHO cells are much more fragile than yeast. Like yeast flocs, CHO flocs can fragment into two, three, or four particles. However, lysis of the individual CHO cells due to the shear stresses created near the stirrer is possible. Kolmogoroff (1941) has shown that the log normal distribution is the asymptotic limit of a repeated breakage process. For floc erosion, Pandya and Spielman (1982) and Lu and Spielman (1985) show that the resulting particles are described by a log normal distribution. Since lysis of CHO cells is more like a random breakage process, the log normal fragment distribution function will also be considered here. Different expressions are given in the literature for the log normal distribution. Here, we use the expression presented by Mochizuki and Zydney (1993). Zydney et al. (1994) provide the appropriate equations to transform between the various forms of the log normal distribution given in the literature. Table 3 also gives other fragment distribution functions that have been shown to permit self-similar solutions for fragmentation processes (Peterson, 1986; Peterson et al., 1985).

### *Computational method*

The computational method used to solve the population balance equation (Eqs. 1 and 2) is similar to that described by Spicer and Pratsinis (1996). The total number of flocs present is divided into several sections for ease of computation (in most cases 30 sections are used). Each section, such as section $i$, is represented by a characteristic volume $u_i$ which is the average volume of the sizes contained in the section. It is assumed that $u_i = 2u_{i-1}$. Thus, Eq. 1 can be written as (Kusters et al., 1993)

$$\begin{aligned}\frac{dV_i}{dt} = &\sum_{j=1}^{i-2} 2^{j-i+1}\alpha_{j(i-1)}\beta_{j(i-1)}V_jV_{i-1} \\ &+ \frac{1}{2}\alpha_{(i-1)(i-1)}\beta_{(i-1)(i-1)}V_{i-1}^2 - V_i\sum_{j=1}^{i-1} 2^{j-i}\alpha_{ji}\beta_{ji}V_j \\ &- V_i\sum_{j=i}^{\max}\alpha_{ji}\beta_{ji}V_j - S_iV_i + \sum_{j=i+1}^{i\max}\Gamma_{i,j}S_jV_j\end{aligned} \tag{5}$$

where $V_i$ is the volume fraction of flocs in section $i$, and $\Gamma_{i,j}$ is the breakage distribution function of size $i$ coming from $j$-sized flocs modified to conserve volume. The upper boundary of the summation in the fourth term is the maximum section number, while the upper boundary of the summation in the sixth term is the largest section number which can produce fragments that fall in section $i$.

Equation 5 can be solved by using a finite-difference approximation. The volume concentration in each section can be calculated from a set of initial conditions. The initial conditions investigated in this article are: initial particle number concentration $9.3\times10^4 - 9.3\times10^7$ cm$^{-3}$, and initial particle diameter 0.5–10 $\mu$m. In addition shear rates between 500 and 50 s$^{-1}$ have been investigated. The solution method used for Eq. 2 is analogous to the method described above for Eq. 1.

In this work we consider only the steady-state solution. Consequently, we do not give details of the dynamic behavior of the system and the time to reach steady state, which do depend on the initial and operating conditions. For the range

**Table 4. Polymer Flocculants Tested**

| No. | Flocculants | Molec. Wt. | Charge Dens. % | Dosage mg Polymer/g Cell | Feedstream |
|---|---|---|---|---|---|
| 1 | CYSEP 2410 | $15-20\times10^6$ | 5 | 0–13 | Yeast |
| 2 | CYSEP 2420 | $15-20\times10^6$ | 10 | 0–14 | Yeast |
| 3 | CYSEP 2440 | $15-20\times10^6$ | 20 | 0–14 | Yeast |
| 4 | CYSEP 2460 | $15-20\times10^6$ | 40 | 0–14 | Yeast |
| 5 | CYSEP 2480 | $15-20\times10^6$ | 55 | 0–18 | Yeast |
| 6 | CYSEP 2454 | $8-12\times10^6$ | 20 | 0–14 | Yeast |
| 7 | CYSEP 2456 | $8-12\times10^6$ | 40 | 0–14 | Yeast |
| 8 | CYSEP 2458 | $8-12\times10^6$ | 55 | 0–17 | Yeast |
| 9 | CYSEP 2461 | $8-12\times10^6$ | 40 | 0–14 | Yeast |
| 10 | CYSEP 2465 | $8-12\times10^6$ | 35 | 0–18 | Yeast |
| 11 | CYSEP 2485 | $5-8\times10^6$ | 55 | 0–18 | Yeast |
| 12 | CYSEP 4218 | $1-5\times10^6$ | 10 | 0–9 (0–850)* | Yeast (CHO cell)* |
| 13 | CYSEP 4224 | $1-5\times10^6$ | 40 | 0–9 | Yeast |
| 14 | CYSEP 4225 | $1-5\times10^6$ | 55 | 0–9 (0–850)* | Yeast (CHO cell) |

*CHO cell concentration was $1-2\times10^6$ cell/mL solution; flocculant dosage for CHO cell feedstream is in ppm.

of initial and operating conditions tested here, a steady-state solution is always obtained.

The fourth-order Runge-Kutta method with adaptive step size control is used to obtain the particle-size distribution at each time step from a given initial condition. The calculation was conducted until steady state was reached. In this study, steady state is defined as follows

$$\epsilon = \left| \frac{d_{V,i} - d_{V,i-1}}{d_{V,i}} \right| < 10^{-6} \tag{6}$$

where $d_{V,i-1}$ and $d_{V,i}$ are the volume based average particle size at time step $i-1$ and $i$, respectively, and $\epsilon$ is the relative difference of the average particle size between two neighboring steps.

## Experimental Methods

Flocculation experiments were conducted using baker's yeast and CHO cell (American Type Culture Collection (ATCC), Manassas, VA, catalogue number CRL-9606) feedstreams. Table 4 summarizes the flocculants used. In the case of baker's yeast, the cells were washed and suspended in deionized water containing glucose. The ratio of glucose to yeast was 1:5. The yeast suspension (25 mL) was then diluted 50% by adding a total of 25 mL of deionized water and 1% polymer solution. The amount of polymer solution added depended on the desired final flocculant concentration. The suspensions were then stirred in a beaker for various times ranging from 1 to 20 min at stirring speeds ranging from 50 to 1,000 rpm, after which the particle-size distribution of the flocculated feedstreams was measured using a Coulter (Miami, FL) LS 230 laser diffraction particle analyzer. The procedure used for the CHO cell experiments was similar except that the cells were suspended in growth medium.

## Results

The population balance Eqs. 1 and 2 were solved using the method described above. Figure 1 gives the results for the four different fragment distribution functions investigated. The collision frequency is given by the Abrahamson equation (Eq. 5, Table 2). In Figure 1, the cumulative volume fraction $F(V_i)$ is plotted as a function of dimensionless floc diameter $d_i/d_V$. The dimensionless floc diameter is defined as a floc diameter $d_i$ divided by the average diameter $d_V$, which is calculated by

$$d_V = \sum_{i=1}^{\max} d_i V_i \tag{7}$$

where $V_i$ is the volume fraction of flocs in section $i$. $d_V$ is the volume based average floc diameter. Figure 2 is analogous except that the cumulative floc number fraction $F(N_i)$ is plotted as a function of dimensionless floc diameter $d_i/d_N$ where $d_N$ is defined by

$$d_N = \sum_{i=1}^{\max} d_i N_i \tag{8}$$

where $N_i$ is the number fraction of flocs in section $i$. $d_N$ is the number based average floc diameter. Shear rates between 500 and 50 $s^{-1}$ were used. All the curves in Figure 1 are independent of shear rate. In Figure 2, for the log normal fragment distribution function, for dimensionless particle di-

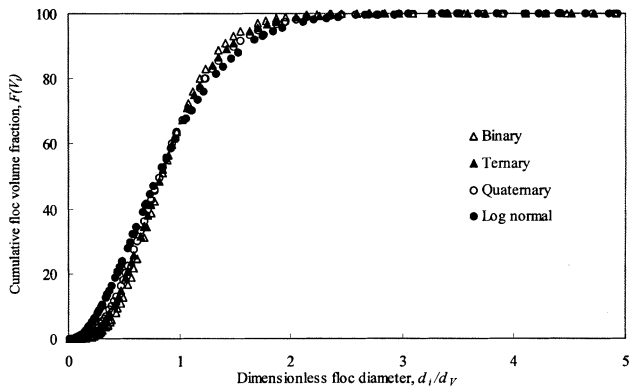


**Figure 1. Cumulative floc volume fraction as a function of dimensionless floc diameter.**

$d_V$ is the volume average floc diameter. Results are shown for binary, ternary, quaternary and log normal fragment distribution functions. The Abrahamson equation (Eq. 5, Table 2) was used for the collision frequency. All curves are for shear rates ranging from 50–500 $s^{-1}$.

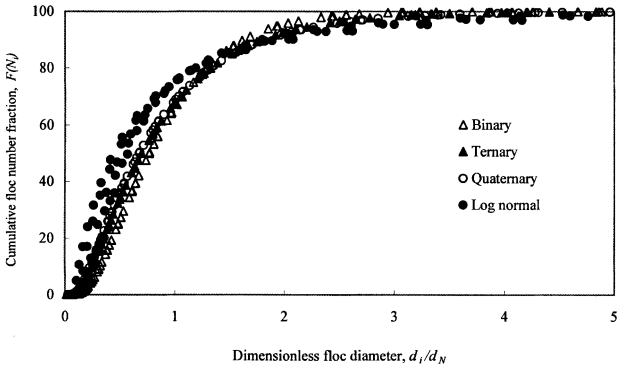


**Figure 2. Cumulative floc number fraction as a function of dimensionless floc diameter.**

$d_N$ is the number average floc diameter. Results are shown for binary, ternary, quaternary and log normal fragment distribution functions. The Abrahamson equation (Eq. 5, Table 2) was used for the collision frequency. All curves are for shear rates ranging from 50–500 $s^{-1}$.

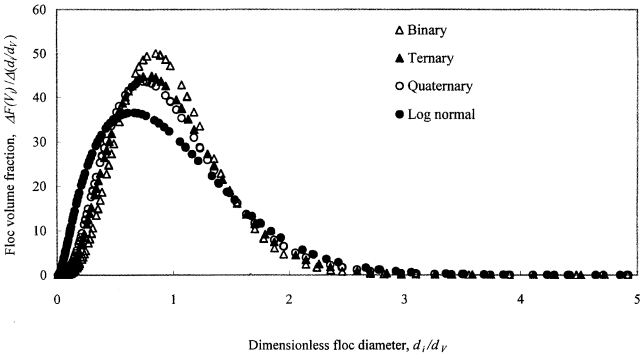


**Figure 3. Floc volume fraction as a function of dimensionless floc diameter.**

$d_V$ is the volume average floc diameter. Results are shown for binary, ternary, quaternary, and log normal fragment distribution functions. The Abrahamson equation (Eq. 5, Table 2) was used for the collision frequency. All curves are for shear rates ranging from 50–500 $s^{-1}$.

ameter less than 2, the results obtained for different shear rates do not fall on the same curve. However, for the binary, ternary, and quaternary fragment distribution functions, the results at different shear rates do appear to fall on the same curve.

Figures 3 and 4 give $\Delta F(V_i)/\Delta(d_i/d_V)$ and $\Delta F(N_i)/\Delta(d_i/d_N)$ vs. dimensionless floc diameter, respectively. These figures plot the derivative of the corresponding cumulative distributions shown in Figures 1 and 2. Again, results are given for the four different fragment distribution functions investigated. In Figure 3, the results are independent of shear rate. However, in Figure 4, for the ternary, quaternary, and log normal fragment distribution functions at smaller dimensionless particle diameters, the results do depend on shear rate. Consequently, results for the different fragment distribution functions are shown separately for clarity. The results in Figures 1–4 were obtained for initial particle number concentrations ranging from $9.3\times10^4$ to $9.3\times10^7$ $cm^{-3}$, and initial particle diameters ranging from 0.5 to 10 $\mu$m. No effect of either initial particle concentration or particle diameter was observed in these ranges.

Figures 1 and 2 show that the cumulative volume and number fractions for the four different fragment distribution functions appear similar. Although Figure 4 shows that the floc number fraction for ternary and quaternary fragment distribution functions deviate from self-similar behavior for smaller floc diameters, this is not evident in the corresponding cumulative distribution shown in Figure 2. Thus, small deviations from self-similar behavior are less easily seen in the cumulative distribution.

Figures 5 and 6 are analogous to Figures 3 and 4 except that the Saffman and Turner equation (Eq. 3 in Table 2) was used to predict the collision frequency. In Figures 5 and 6 each of the distribution functions corresponding to the different fragment distribution functions are shown separately for clarity. Data are shown for shear rates from 500–50 $s^{-1}$. Figure 5 gives the variation of the floc volume fraction with the dimensionless floc diameter. As can be seen with the exception of the binary fragment distribution function, the shear rate does affect the shape of the floc volume fraction curves at smaller dimensionless particle diameters. In the case of Figure 6, which gives the floc number fraction, the shear rate affects the shape of the curves for all four fragment distribution functions. The results in Figures 5–6 were obtained for initial particle number concentrations ranging from $9.3\times10^4$ to $9.3\times10^7$ $cm^{-3}$, and initial particle diameters ranging from 0.5 to 10 $\mu$m. No effect of either initial particle concentration or particle diameter was observed in these ranges.

Figures 7–10 show the corresponding experimental data. Figure 7 gives the variation of the cumulative floc volume fraction as a function of dimensionless particle diameter. Results for yeast and CHO cells are plotted as solid and dashed lines, respectively, and are shown separately for clarity. Numerical results for the binary and log normal fragment distribution functions are also shown as solid lines with open squares and triangles, respectively. Figure 8 gives the experimentally determined cumulative floc number fraction for yeast and CHO cells together with numerical results for the binary and log normal distribution functions. In Figures 7 and 8, the collision frequency was given by the Abrahamson equation for the numerical results.

Figures 9 and 10 give the floc volume and number fraction, respectively. Results for yeast and CHO cells are plotted as solid and dashed lines, respectively, and are shown separately for clarity. Numerical results for the binary and log normal fragment distribution functions are included as solid lines with open squares and triangles, respectively. The collision frequency was given by the Abrahamson equation for the numerical results. From Figure 4, when the log normal fragment distribution is used, the floc number fraction depends on shear rate. In Figure 10, the numerical result for the log normal fragment distribution function is for a shear rate of 500 $s^{-1}$.

## Discussion

The conditions necessary for the existence of a steady-state particle-size distribution when flocculation and fragmentation occur simultaneously have been discussed in detail by Vigil and Ziff (1989) and Ramkrishna (2000). Since the rates

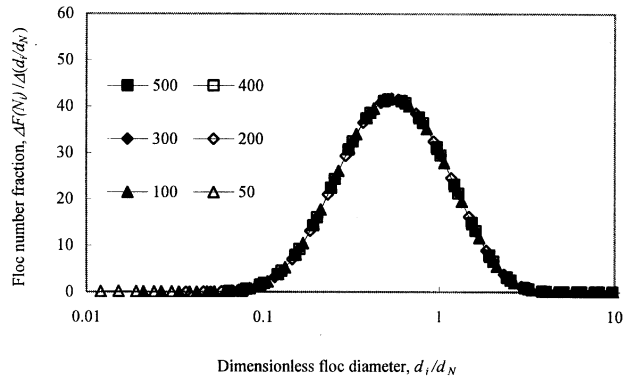


(a) Binary fragment distribution function

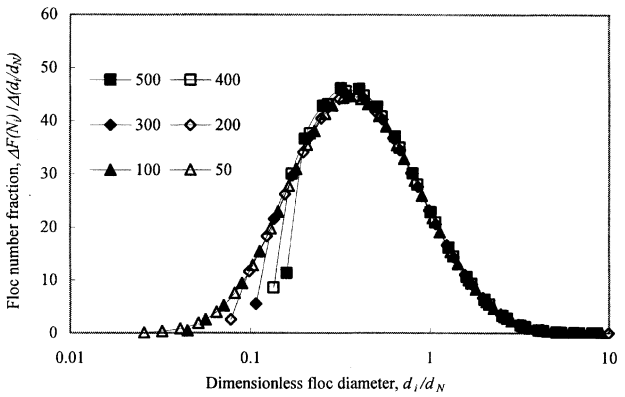


(c) Quaternary fragment distribution function

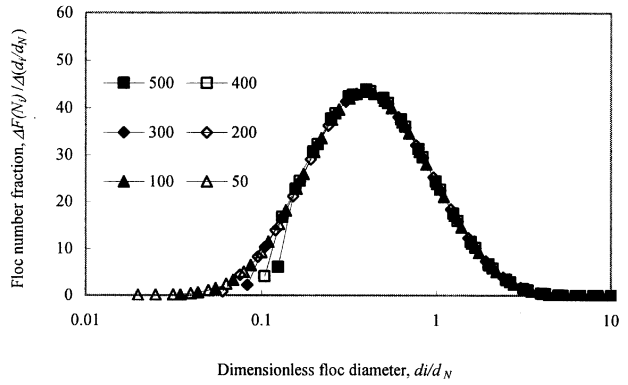


(b) Ternary fragment distribution function

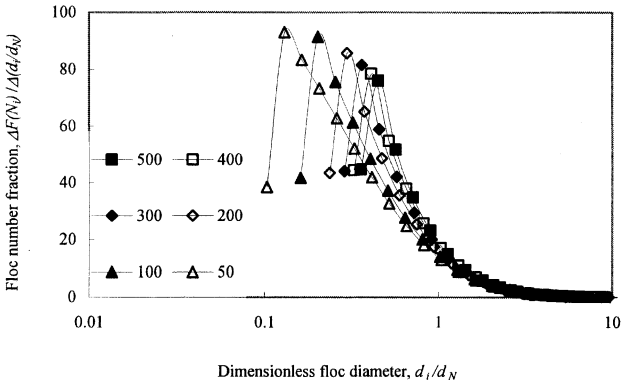


(d) Log normal fragment distribution function

**Figure 4. Floc number fraction as a function of dimensionless floc diameter.**

$d_N$ is the number average floc diameter. Results are shown for binary, ternary, quaternary and log normal fragment distribution functions. The Abrahamson equation (Eq. 5, Table 2) was used for the collision frequency. Shear rates shown in the legends are in $s^{-1}$.

of flocculation ( $\beta_{jk}$ and $\beta'_{jk}$) and fragmentation ($S_i$ and $S'_i$) depend on the size of the particles present, it is possible that a particle-size distribution exists where the time scales of the two processes can match each other leading to a steady-state particle-size distribution. In general, larger particles fragment more easily than smaller particles. Ramkrishna (2000) also discusses the necessary conditions for self-similar behavior if a steady-state particle-size distribution exists. A cumulative distribution such as $F(V_i)$ and $F(N_i)$ will be self-similar if the corresponding distribution functions $\Delta F(V_i)/\Delta(d_i/d_V)$ and $\Delta F(N_i)/\Delta(d_i/d_N)$ are self-similar.

Previous investigators have shown that use of fragmentation rates of the form of Eqs. 3 or 4 (Ramkrishna, 2000; Kapur, 1972; Peterson, 1986; Peterson et al., 1985) and binary, ternary, quaternary, or log normal fragment distribution functions could lead to a self-similar solution. Earlier studies (Pearson et al., 1984; Spicer and Pratsinis, 1996; Spicer et al., 1996a) have also shown that use of the Saffman and Turner equation (Eq. 3, Table 2) could lead to a self-similar particle-size distribution.

Figures 1 and 2 show the cumulative floc volume and number fractions as a function of volume and number based average particle diameter. Kapur (1972) and Ramkrishna (2000) show that scaling the particle diameter by the average particle diameter could lead to the existence of a self-similar solution. Figure 1 shows that the cumulative floc volume curves for shear rates from 50–500 $s^{-1}$ lead to self-similar solutions for the four fragment distribution functions investigated. Figure 2 shows that, for the log normal fragment distribution function, the numerical data points for dimensionless particle diameters less than 2, obtained at different shear rates, do not fall on the same curve. Consequently, it appears that with the exception of the log normal fragment distribution function self-similar solutions appear to exist for binary, ternary, and quaternary fragmentation.

Since the cumulative distribution functions shown in Figure 1 are self-similar, we would expect the distribution functions themselves to be self-similar. Figure 3 shows that this is in fact the case.

Figure 4 shows the distribution functions given by the four fragment distribution functions plotted against dimensionless particle diameter that correspond to the various cumulative distribution functions shown in Figure 2. As can be seen, only binary fragmentation leads to a self-similar solution for all

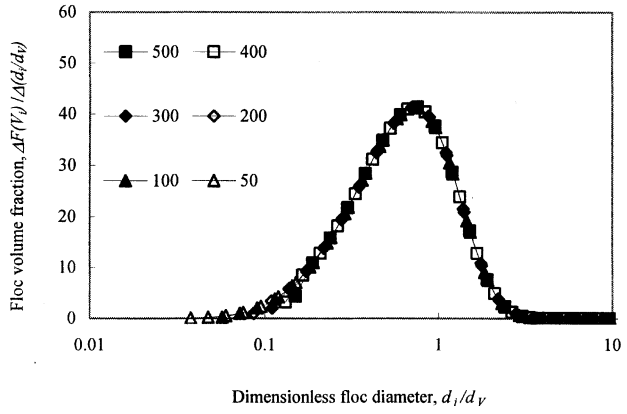


(a) Binary fragment distribution function

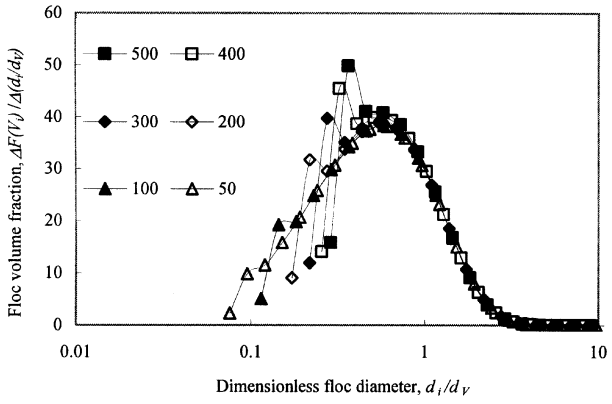


(c) Quaternary fragment distribution function

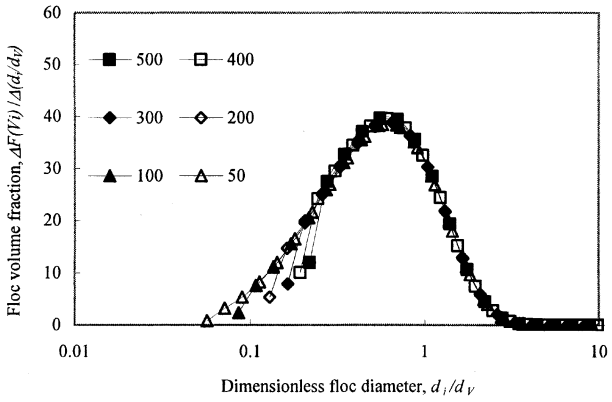


(b) Ternary fragment distribution function

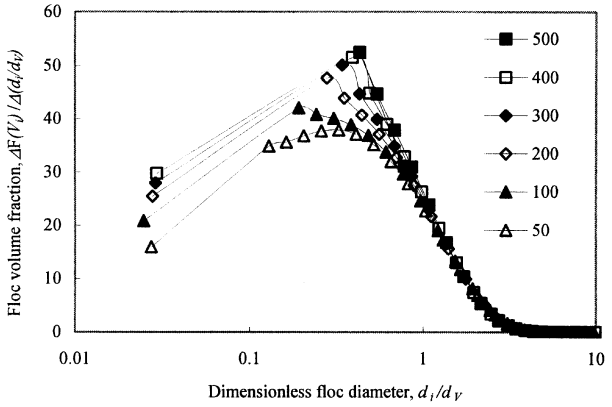


(d) Log normal fragment distribution function

**Figure 5. Floc volume fraction as a function of dimensionless floc diameter.**

$d_V$ is the volume average floc diameter. Results are shown for binary, ternary, quaternary, and log normal fragment distribution functions. The Saffman and Turner equation (Eq. 3, Table 2) was used for the collision frequency. Shear rates shown in the legends are in $s^{-1}$.

floc diameters. Deviations from self-similarity are observed for shear rates above 300 $s^{-1}$ for ternary fragmentation, above 200 $s^{-1}$ for quaternary fragmentation and at all shear rates investigated for log normal fragment distribution function.

As can be seen from Figure 5, only the binary fragment distribution appears to lead to a self-similar solution (for all floc diameters) for the floc volume fraction at all the shear rates investigated. In fact, closer investigation of the result for binary fragmentation showed small deviations from self-similarity at a shear rate of 500 $s^{-1}$. For the ternary fragment distribution function, deviations from self-similarity are observed at shear rates above 200 $s^{-1}$ and, for the quaternary and log normal fragment distribution functions, self-similarity for all floc diameters was not observed for any of the shear rates investigated. Figure 6 shows that self-similar solutions were not found to exist over the entire range of floc diameters for all four fragment distribution functions.

The results shown in Figures 5 and 6 are in agreement with similar calculations performed by Spicer and Pratsinis (1996). These authors point out that the shape of the steady-state floc size distribution is not affected by shear rate (for a given fragment distribution function) once the flocs grow well beyond the size of the initial particles. At higher shear rates, Figures 4–6 show that the floc volume and number distribution functions are self-similar for larger floc diameters. However, at smaller floc diameters and at higher shear rates, deviations from self-similarity are observed. As the particles start to grow, since the collision frequency given by the Saffman and Turner and Abrahamson equations increases with increasing particle size, the rate of flocculation increases. However, at high shear rates, when a large number of primary particles are present, flocculation of the particles is suppressed; hence, full self-similarity over all floc diameters is not obtained. Nevertheless, all the distributions shown in Figures 4–6 are steady-state distributions.

Comparing Figures 3 and 4 with 5 and 6, we see that the collision frequency equation used does have a significant effect on the floc volume and number fraction curves. In par-

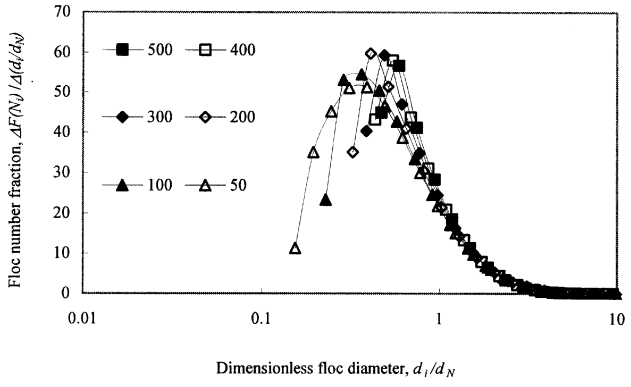


(a) Binary fragment distribution function

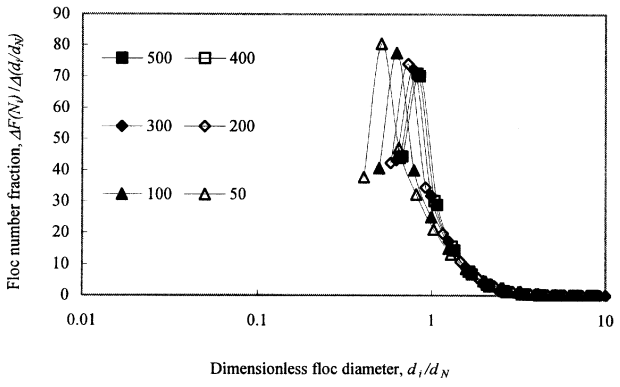


(c) Quaternary fragment distribution function

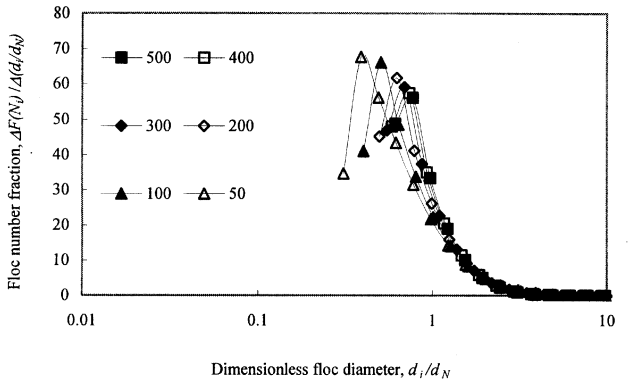


(b) Ternary fragment distribution function

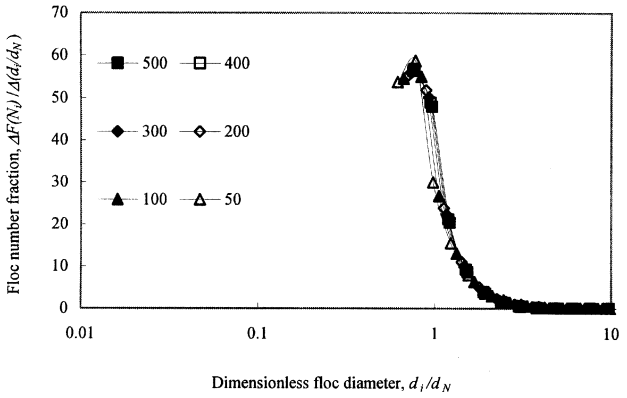


(d) Log normal fragment distribution function

**Figure 6. Floc number fraction as a function of dimensionless floc diameter.**

$d_N$ is the number average floc diameter. Results are shown for binary, ternary, quaternary, and log normal fragment distribution functions. The Saffman and Turner equation (Eq. 3, Table 2) was used for the collision frequency. Shear rates shown in the legends are in $s^{-1}$.

ticular, if the collision frequency is predicted by the Abrahamson equation, self-similarity is found to exist at higher shear rates for a given fragment distribution function compared to the Saffman and Turner equation. Further, Figures 4–6 also show that the maximum shear rate at which self-similar solutions exist decreases with fragment distribution function in the order binary, ternary, quaternary, and log normal. This is true irrespective of whether the collision frequency is given by the Saffman and Turner or Abrahamson equations.

The log normal fragment distribution function will produce more smaller fragments than the quaternary fragment distribution function. Similarly, the ternary fragment distribution function will produce less small fragments than the quaternary fragment distribution function. The binary fragment distribution function will produce two approximately equal fragments. At higher shear rates, flocculation of smaller fragments is suppressed. Thus, fragment distribution functions that produce more small particles will deviate from the self-similar solution for small floc diameters, at higher shear rates.

The experimental results for yeast and CHO cells are given in Figures 7–10. Figures 7 and 8 indicate that the experimentally determined cumulative floc volume and number fractions appear to show self-similar behavior. In Figures 7–10 numerical results for the binary and log normal fragment distribution functions using the Abrahamson equation for the collision frequency are also shown. For the log normal distribution, values of $\sigma$ ranging from 2 to 20 were investigated. In Figures 7–10, $\sigma = 12$ is used since this value was found to give the best fit to the experimental data.

Figure 9 shows that within experimental uncertainty the floc volume fraction for yeast and CHO cells show self-similar behavior. Since only the numerical results obtained using the Abrahamson equation for the collision frequency show self-similar behavior for all dimensionless floc diameters, the numerical results obtained using the Saffman and Turner equation were not used to model the experimental results. Further, from Figures 7 and 9, it can be seen that the binary fragment distribution gives the best prediction of the results for yeast, while the log normal fragment distribution function gives the best prediction for CHO cells. This is in keeping with our hypothesis that yeast flocs are likely to fragment into two particles where, as CHO cells, they could lyse pro-

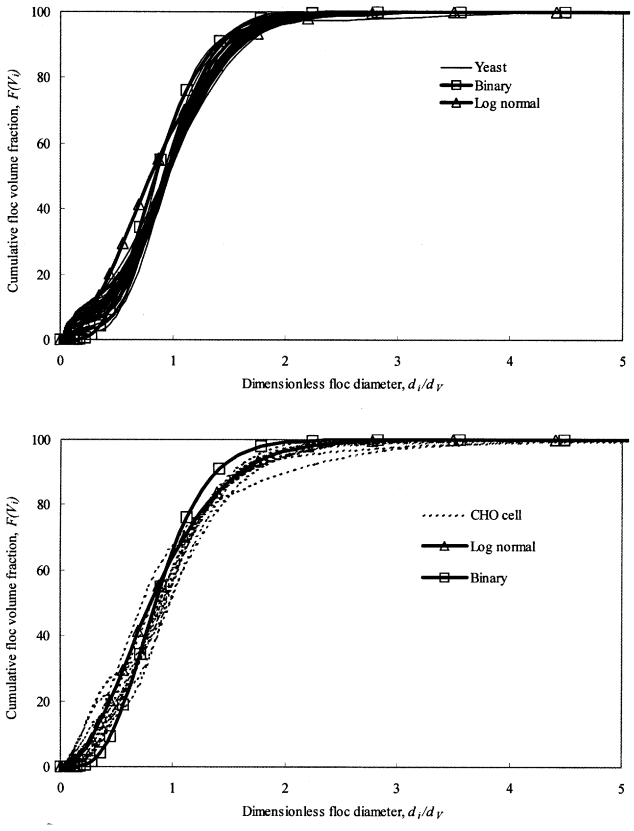


**Figure 7. Cumulative floc volume fraction as a function of dimensionless floc diameter.**

$d_V$ is the volume average floc diameter. Solid lines are experimental results for yeast, dashed lines are experimental results for CHO cells. Open squares and triangles represent the numerical results using binary and log normal fragment distribution functions, respectively. The Abrahamson equation (Eq. 5, Table 2) was used for the collision frequency.

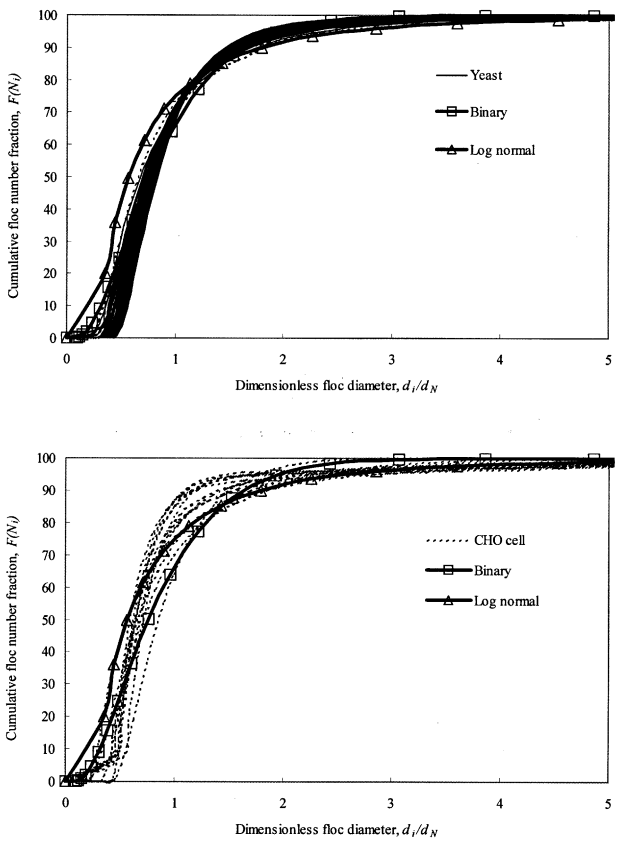


**Figure 8. Cumulative floc number fraction as a function of dimensionless floc diameter.**

$d_N$ is the number average floc diameter. Solid lines are experimental results for yeast, dashed lines are experimental results for CHO cell. Open squares and triangles represent the numerical results using binary and log normal fragment distribution functions, respectively. The Abrahamson equation (Eq. 5, Table 2) was used for the collision frequency.

ducing a greater range of smaller particles that may be described by a log normal distribution.

Figure 10 shows that within experimental uncertainty, the floc number fraction for yeast and CHO cells also show self-similar behavior. Since using the Abrahamson equation to predict the collision frequency is more likely to result in self-similar behavior over a greater range of floc diameters, the numerical results obtained using the Saffman and Turner equation were not used to model the experimental results. Like Figure 9, numerical results for the binary and log normal fragment distribution function are shown.

In Figure 9, the experimental results for yeast and CHO cells are well predicted by the numerical results using the binary and log normal fragment distribution functions, respectively. In Figure 10, however, the experimental results for yeast and CHO cells are similar: both are predicted better by the log normal fragment distribution function. For CHO cells, this is not surprising since the floc volume fraction was also predicted best by the log normal fragment distribution function.

The results for yeast in Figure 10 do not agree with the results shown in Figure 9. Kim et al. (2001) have shown that baker's yeast contains a significant amount of sub-micron sized small cell debris. The percentage by volume of this sub-micron sized particulate matter is small. However, the number of sub-micron sized particles is large. Thus, it could be that this sub-micron sized particulate matter contributes significantly to the floc number fraction, hence, the log normal fragment distribution function gives a better prediction of the experimental data than the binary fragment distribution function.

In this work we have used the log normal distribution to describe the fragment distribution function. However, this is not the only choice. For example, we could have used a truncated normal distribution instead. In fact any function that permits the existence of a self-similar solution could be used (see Table 3). We choose the log normal distribution since it is the asymptotic limit of a repeated breakage process (Kolmorogov, 1941).

We present our experimental and numerical results in terms of a dimensionless floc diameter. All the flocculants given in Table 4 were tested using yeast cells. However, as indicated in Table 4, only two of these flocculants were used to flocculate CHO cells. For all of the experimental conditions tested, we found self-similar behavior. Obtaining a self-

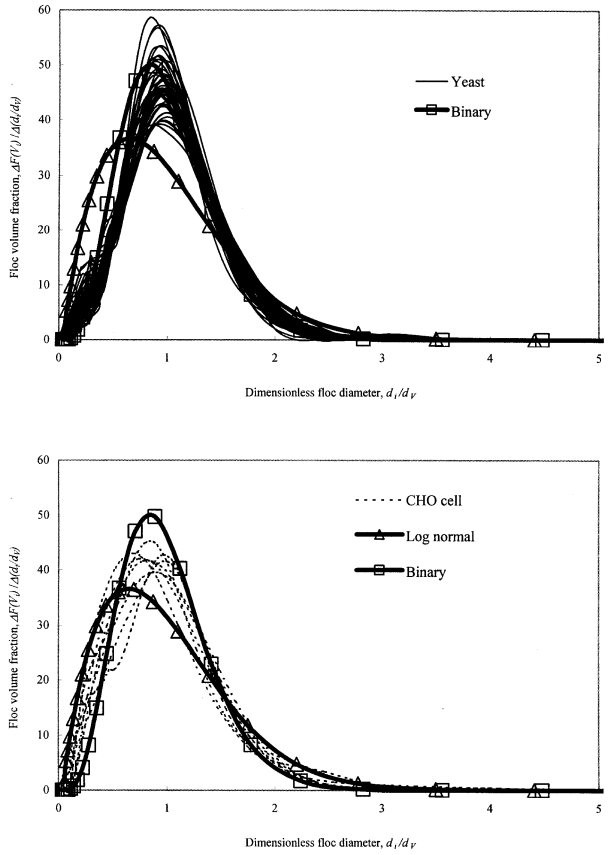


**Figure 9. Floc volume fraction as a function of dimensionless floc diameter.**

$d_V$ is the volume average floc diameter. Solid lines are experimental results for yeast, dashed lines are experimental results for CHO cell. Open squares and triangles represent the numerical results using binary and log normal fragment distribution functions, respectively. The Abrahamson equation (Eq. 5, Table 2) was used for the collision frequency.

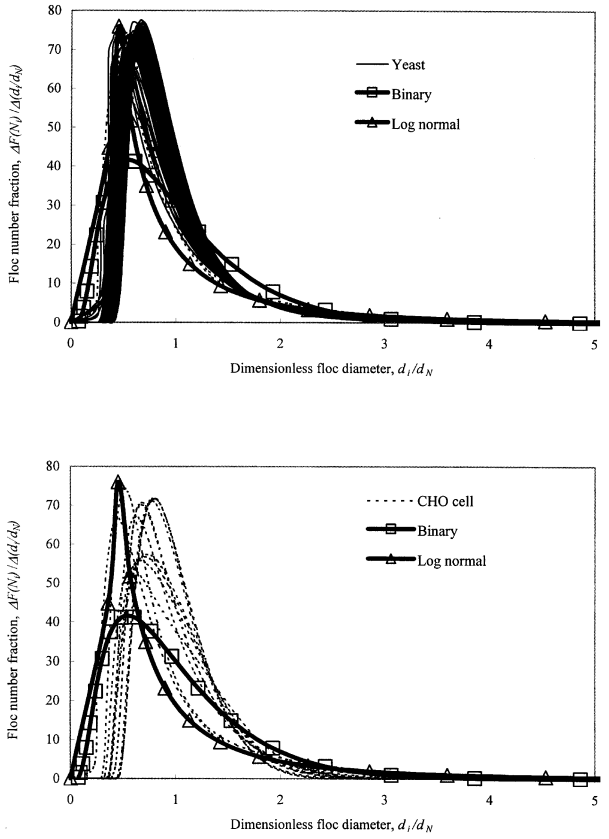


**Figure 10. Floc number fraction as a function of dimensionless floc diameter.**

$d_N$ is the number average floc diameter. Solid lines are experimental results for yeast, dashed lines are experimental results for CHO cell. Open squares and triangles represent the numerical results using binary and log normal fragment distribution functions, respectively. The Abrahamson equation (Eq. 5, Table 2) was used for the collision frequency. The shear rate for the log normal distribution function was 500 $s^{-1}$.

similar steady-state floc size distribution is of considerable value in characterizing the experimental results. Our numerical results also exhibit self-similar behavior over a range of initial and operating conditions. This is not surprising since the functional forms used for $\alpha_{jk}$, $\beta_{jk}$, $S_i$, $\gamma_{ij}$, $\alpha'_{jk}$, $\beta'_{jk}$, $S'_i$ and $\gamma'_{ij}$ and the definition of the dimensionless floc size can be shown mathematically to permit the existence of a self-similar size distribution (Ramkrishna, 2000). However, the actual existence of a self-similar solution is not guaranteed for all initial and operation conditions. Ramkrishna (2000) discusses this point in detail.

The experimental and numerical results indicate that the average particle size and the particle-size distribution at steady state do depend on the initial conditions and operating conditions. For flocculation of biological cells, this is described in our earlier publications (Kim et al., 2001; Wickramasinghe et al., 2002). We obtain good agreement between experimental and numerical results (Figures 7–10) when compared in terms of dimensionless floc diameter. Table 5 gives the actual numerically and experimentally determined volume based average floc size for the range of conditions

**Table 5. Comparison of Actual Numerical and Experimental Steady-State Particle-Size Distributions and Volume Based Average Particle Size***

| | Numerical | Yeast | CHO Cell |
|---|---|---|---|
| Shear rate ($s^{-1}$) | 50–500 | 2–200 | 40 |
| Initial particle diameter ($\mu$m) | 0.5–10 | 8–9 | 10 |
| Initial particle concentration (cells/$cm^3$) | $9.3\times10^4$–$9.3\times10^7$ | $5\times10^7$ | $1$–$2\times10^6$ |
| Steady-state particle-size range ($\mu$m) | 0.5–$1.0\times10^4$ | 0.4–2,000 | 0.4–260 |
| Volume based average particle size ($\mu$m) | 1–2,000 | 10–700 | 15–70 |

*The experimental results fall within the range of numerical results.

investigated. In our study with the exception of the shear rate, numerical conditions were chosen in order to bracket the conditions used experimentally. For the numerical results at shear rates less than 50 $s^{-1}$, obtaining a steady-state solution often took a very long time. Consequently, results reported here are only for shear rates between 50–500 $s^{-1}$. As can be seen, the experimentally determined average particle sizes do fall within the range of values obtained numerically.

Direct comparison of the actual floc diameters obtained experimentally and numerically is not straightforward. During the simulation, the system is subjected to a constant uniform shear rate. However, in the experimental system, since a magnetic stirrer is used, a range of shear rates exists. In Table 5 the shear rate was estimated using the method described by Spicer et al. (1996b) for stirred tanks.

Actual flocs are not spherical in both the experimental and numerical systems. Commercially available particle sizers transform the scatter patterns obtained into an expected particle-size distribution using theories such as those of Mie (Stover, 1990) assuming spherical particles. However, in the simulation the diameter of a given floc is calculated as follows: first, the total volume of the floc is calculated based on the number of the primary particles in the floc, then the diameter is calculated from the total volume assuming that the floc is a sphere. Although the particle sizer is accurate to about 1% of the average particle size (Coulter Co., 1994), average floc diameters determined experimentally and numerically will be different. Further, our particle sizer can only measure flocs in the size range 0.4–2,000 $\mu$m. Flocs outside this range will not be reported correctly. These differences are minimized by presenting results in terms of the dimensionless floc diameter, as defined by Eqs. 7 and 8.

The results obtained here show that a population balance equation may be used to model floc size distributions for yeast and CHO cells. The numerical results show that a self-similar particle-size distribution may not always be obtained. In order to improve the permeate flux during microfiltration it is essential to minimize the amount of small particulate matter and cell debris present (Kim et al., 2001). Consequently, the stirring conditions (shear stress and time) may be important. The results obtained here could be used to help guide the selection of appropriate flocculation conditions for practical applications.

## Conclusions

A population balance model has been used to predict the floc size distribution for feedstreams of yeast and CHO cells. The floc volume fraction for yeast cells is predicted best by the binary fragment distribution function, but the floc number fraction is predicted best by the log normal fragment distribution function. For CHO cells, the log normal fragment distribution function gives the best prediction for the floc volume and number fraction.

Using the equation by Abrahamson for the collision frequency gives better predictions of the experimental results than the equation by Saffman and Turner. Further self-similar behavior is observed at higher shear rates for the Abrahamson equation. Since minimizing the amount of smaller particulate matter present could enhance the permeate fluxes during microfiltration, flocculation of cells at shear rates that lead to self-similar floc size distributions may be beneficial.

## Acknowledgments

Financial support for this research was obtained from the National Science Foundation (CAREER Program Grant No. BES 9984095). The authors wish to thank Yanling Wu for her assistance in conducting some of the experiments. This article is dedicated in memory of Dr. Rajiv Bhadra.

## Notation

$a$ = principal rate of strain in Eq. 1, Table 1; parameter in Eq. 7, Table 3
$A$ = specific fragmentation rate for the largest particles present in Eq. 3
$A'$ = proportionality constant in Eq. 4
$B$ = cumulative breakage distribution function in Eq. 4, Table 3
$c$ = parameter in Eq. 2, Table 1, Eq. 1, Table 3 and Eq. 7, Table 3
$d$ = diameter of flocs; parameter in Eq. 7, Table 3
$F$ = cumulative fraction of flocs
$F_c$ = collision diameter function in Eq. 4, Table 2
$G$ = shear rate
$k$ = Boltzmann constant in Eq. 1, Table 2
$K$ = variable in Eq. 12, Table 3
$n$ = number fraction of flocs; parameter in Eqs. 9 and 11, Table 3
$N$ = number fraction of floc sections
$r$ = parameter in Eq. 6, Table 3
$s$ = initial dimensionless distance between two particles in Eq. 1, Table 1
$S, S'$ = fragmentation rate of particles
$t$ = time
$T$ = absolute temperature in Eq. 1, Table 2
$u$ = volume of particles
$\overline{U^2}$ = mean squared velocity deviation in Eq. 5, Table 2
$\nu$ = volume fraction of particles
$V$ = volume fraction of floc sections

### *Greek letters*

$\alpha, \alpha'$ = collision efficiency between two colliding particles
$\alpha_o$ = intrinsic efficiency factor in Eq. 2, Table 1
$\beta, \beta'$ = collision frequency between two particles
$\gamma, \gamma'$ = fragment distribution function
$\Gamma$ = breakage distribution function modified to conserve volume
$\delta, \delta', \delta''$ = constant in Eqs. 3 and 4
$\epsilon$ = energy dissipation rate per unit mass in Eq. 5, Table 2; relative difference of the average particle size between two neighboring steps in Eq. 6
$\theta^*$ = characteristic angle in Eq. 1, Table 1
$\mu$ = viscosity in Eq. 1, Table 2
$\sigma$ = standard deviation for the log normal and normal distributions in Eqs. 2, 3, 10, and 12, Table 3
$\tau$ = particle relaxation time in Eq. 5, Table 2

### *Subscripts:*

$i, j, k$ = particles or floc sections number
N = number based
m = mean
max = maximum
V = volume based

## Literature Cited

Abrahamson, J., "Collision Rates of Small Particles in a Vigorously Turbulent Fluid," *Chem. Eng. Sci.*, **30**, 1371 (1975).
Aunins, J. G., and D. I. C. Wang, "Induced Flocculation of Animal Cells in Suspension Culture," *Biotechnol. Bioeng.*, **34**, 629 (1989).

Baran, A. A., "Flocculation of Cellular Suspensions by Polyelectrolytes," *Colloid. Surface*, **31**, 259 (1988).
Batterham, R. J., J. S. Hall, and G. Barton, "Pelletizing Kinetics and Simulation of Full-scale Balling Circuits," *Proc. of 3rd Int. Symp. on Agglomeration*, Nürnberg, Germany, A136, (1981).
Belfort, G., R. H. Davis, and A. L. Zydney, "The Behavior of Suspensions and Macromolecular Solutions in Crossflow Microfiltration," *J. Memb. Sci.*, **96**, 1 (1994).
Bell, D. J., and R. J. Davies, "Cell Harvesting of Oleaginous Yeast by Cross-Flow Filtration," *Biotechnol. Bioeng.*, **29**, 1176 (1987).
Belter, P. A., E. L. Cussler, and W. S. Hu, *Bioseparations: Downstream Processing for Biotechnology*, Wiley, New York (1988).
Berlin, A. A., I. M. Solomentseva, and V. N. Kiskenko, "Suspension Flocculation by Polyelectrolytes: Experimental Verification of a Developed Mathematical Model," *J. Colloid Interf. Sci.*, **191**, 273 (1997).
Blatz, P. J., and A. V. Tobolsky, "Note on the Kinetics of Systems Manifesting Simultaneous Polymerization-Depolymerization Phenomena," *J. Phys. Chem.-US*, **49**, 77 (1954).
Boadway, J. D., "Dynamics of Growth and Breakage of Alum Floc in Presence of Fluid Shear," *J. Environ. Eng. Div.-ASCE*, **104**, 901 (1978).
Broadbent, S. R., and T. G. Callcott, "Coal Breakage Processes I. A New Analysis of Coal Breakage Processes," *J. Inst. Fuel*, **29**, 524 (1956).
Camp, T. R., and P. C. Stein, "Velocity Gradients and Internal Work in Fluid Motion," *J. Boston Soc. Civil Engrs.*, **30**, 219 (1943).
Chellam, S., and M. R. Wiesner, "Evaluation of Crossflow Filtration Models Based on Shear-induced Diffusion and Particle Adhesion: Complications Induced by Feed Suspension Polydispersity," *J. Memb. Sci.*, **138**, 83 (1998).
Chin, C-J., S. Yiacoumi, and C. Tsouris, "Shear-induced Flocculation of Colloidal Particles in Stirred Tanks," *J. Colloid Interf. Sci.*, **206**, 532 (1998).
Coulaloglou, C. A., and L. L. Tavlarides, "Description of Interaction Processes in Agitated Liquid-liquid Dispersions," *Chem. Eng. Sci.*, **32**, 1289 (1977).
Coulter Co., *Coulter LS Series Product Manual*, Coulter Co., Miami, FL (1994).
Danov, K. D., I. B. Ivanov, T. D. Gurkov, and R. P. Borwankar, "Kinetic Model for the Simultaneous Processes of Flocculation and Coalescence in Emulsion Systems," *J. Colloid Interf. Sci.*, **167**, 8 (1994).
Dharmappa, H. B., J. Vernik, R. Ben Aïm, K. Yamamoto, and S. Vigneswaran, "A Comprehensive Model for Cross-Flow Filtration Incorporating Polydispersity of the Influent," *J. Memb. Sci.*, **65**, 173 (1992).
Friedlander, S. K., *Smoke, Dust and Haze*, Wiley, New York (1977).
Gasner, L. L., and D. I. C. Wang, "Microbial Cell Recovery Enhancement through Flocculation," *Biotechnol. Bioeng.*, **12**, 837 (1970).
Gaudin, A. M., and T. P. Meloy, "Model and a Comminution Distribution Equation for Single Fracture," *T. Soc. Min. Eng.*, **223**, 40 (1962).
Gelbard, F., and T. W. Peterson, "Simulation of Aerosol Fragmentation Dynamics," *Aerosol Sci. Tech.*, **2**, 202 (1983).
Hounslow, M. J., R. L. Ryall, and V. R. Marshall, "A Discretized Population Balance for Nucleation, Growth, and Aggregation," *AIChE J.*, **34**, 1821 (1988).
Hughes, J., D. K. Ramsden, and K. C. Symes, "The Flocculation of Bacteria using Cationic Synthetic Flocculants and Chitosan," *Biotechnol. Tech.*, **4**, 55 (1990).
Huisman, I. H., G. Trägårdh, and C. Trägårdh, "Particle Transport in Crossflow Microfiltration II. Effects of Particle-particle Interactions," *Chem. Eng. Sci.*, **54**, 281 (1999).
Kapur, P. C., "Self-Preserving Size Spectra of Comminuted Particles," *Chem. Eng. Sci.*, **27**, 425 (1972).
Kim, J. S., S. Akeprathumchai, and S. R. Wickramasinghe, "Flocculation to Enhance Microfiltration," *J. Memb. Sci.*, **182**, 161 (2001).
Kislenko, V. N., "Mathematical Model of Polymer Adsorption Accompanied by Flocculation," *J. Colloid Interf. Sci.*, **226**, 246 (2000).
Koh, P. T. L., J. R. G. Andrews, and P. H. T. Uhlherr, "Modelling Shear-flocculation by Population Balances," *Chem. Eng. Sci.*, **42**, 353 (1987).
Kolmogoroff, A. N., "Über das Lograthimisch Normale Verteilungsgesetz der Dimensionen der Teilchen bei Zerstückelung," *C. R. Acad. Sci. (Doklady) URSS*, **XXX1**, 99 (1941).
Kusters, K. A., S. E. Pratsinis, S. G. Thoma, and D. M. Smith, "Ultrasonic Fragmentation of Agglomerate Powders," *Chem. Eng. Sci.*, **48**, 4119 (1993).
Lu, C. F., and L. A. Spielman, "Kinetics of Floc Breakage and Aggregation in Agitated Liquid Suspensions," *J. Colloid Interf. Sci.*, **103**, 95 (1985).
McAnally, W. H., and A. J. Mehta, "Aggregation Rate of Fine Sediment," *J. Hydraulic Eng.*, **126**, 883 (2000).
Mochizuki, S., and A. L. Zydney, "Theoretical Analysis of Pore Size Distribution Effects on Membrane Transport," *J. Memb. Sci.*, **82**, 211 (1993).
Ofsthun, N. J., "Cross-flow Membrane Filtration of Cell Suspensions," PhD Thesis, MIT, Cambridge, MA (1989).
Oles, V., "Shear-Induced Aggregation and Breakup of Polystyrene Latex-Particles," *J. Colloid Interf. Sci.*, **154**, 351 (1992).
Pandya, J. D., and L. A. Spielman, "Floc Breakage in Agitated Suspensions: Theory and Data Processing Strategy," *J. Colloid Interf. Sci.*, **90**, 517 (1982).
Patel, P. N., M. A. Mehaia, and M. Cheryan, "Cross-Flow Membrane Filtration of Yeast Suspensions," *J. Biotechnol.*, **5**, 1 (1987).
Pearson, H. J., I. A. Valioulis, and E. J. List, "Monte-carlo Simulation of Coagulation in Discrete Particle-size Distributions 1. Brownian-motion and Fluid Shearing," *J. Fluid Mech.*, **143**, 367 (1984).
Peng, S. J., and R. S. Williams, "Direct Measurement of Floc Breakage in Flowing Suspensions," *J. Colloid Interf. Sci.*, **166**, 321 (1994).
Peterson, T. W., *Proc. Aerosol Conf.*, B. Y. H. Liu, D. Y. H. Pui, and H. J. Fissan, eds., First International Aerosol Conference, Minneapolis, MN, Elsevier, New York, 760 (Sept. 17-21, 1984).
Peterson, T. W., "Similarity Solutions for the Population Balance Equation Describing Particle Fragmentation," *Aerosol Sci. Tech.*, **5**, 93 (1986).
Peterson, T. W., M. V. Scotto, and A. F. Sarofim, "Comparison of Comminution Data with Analytical Solutions of the Fragmentation Equation," *Powder Technol.*, **45**, 87 (1985).
Ramkrishna, D., *Population Balances: Theory and Applications to Particulate Systems in Engineering*, Academic Press, New York (2000).
Randolph, A. D., and R. Ranjan, "Effect of a Material-Flow Model in Prediction of Particle-size Distributions in Open- and Closed-Circuit Mills," *Int. J. Mineral Process.*, **4**, 99 (1977).
Ray, D. T., and R. Hogg, "Agglomerate Breakage in Polymer-flocculated Suspensions," *J. Colloid Interf. Sci.*, **116**, 256 (1987).
Reich, I., and R. D. Vold, "Flocculation-Deflocculation in Agitated Suspension I. Carbon and Ferric Oxide in Water," *J. Phys. Chem.-US*, **63**, 1497 (1959).
Reid, K. J., "A Solution to Batch Grinding Equation," *Chem. Eng. Sci.*, **20**, 953 (1965).
Russotti, G., A. E. Osawa, R. D. Sitrin, B. C. Buckland, W. R. Adams, and S. S. Lee, "Pilot-scale Harvest of Recombinant Yeast Employing Microfiltration: A Case Study," *J. Biotechnol.*, **42**, 235 (1995).
Saffman, P. G., and J. S. Turner, "On the Collision of Drops in Turbulent Clouds," *J. Fluid Mech.*, **1**, 16 (1956).
Shamlou, P. A., and N. Tichener-Hooker, "Turbulent Aggregation and Breakup of Particles in Liquids in Stirred Vessels," *Processing of Solid Liquid Suspensions*, P. A. Shamlou, ed., Butterworth Heinemann, Oxford (1993).
Shoji, K., S. Lohrasb, and L. G. Austin, "Variation of Breakage Parameters with Ball and Powder Loading in Dry Ball Milling," *Powder Technol.*, **25**, 109 (1980).
Silk, J., *Star Formation*, Geneva Observatory, Sauverny, Switzerland (1980).
Smoluchowski, M., "Drei Vorträge über Diffusion brownsche Bewegung und Koagulation von Kolloidteilchen," *Physik Z.*, **17**, 557 (1916).
Smoluchowski, M., "Versuch einer Mathematischen Theorid der Koagulationskinetic kolloider Lösungen," *Z. Phys. Chem.*, **92**, 129 (1917).
Spicer, P. T., and S. E. Pratsinis, "Coagulation and Fragmentation: Universal Steady-state Particle Size Distribution," *AIChE J.*, **42**, 1612 (1996).
Spicer, P. T., S. E. Pratsinis, and M. D. Trennepohl, "Coagulation and Fragmentation: The Variation of Shear Rate and the Time

Lag for Attainment of Steady State," *Ind. Eng. Chem. Res.*, **35**, 3074 (1996a).
Spicer, P. T., W. Keller, and S. E. Pratsinis, "The Effect of Impeller Type on Floc Size and Structure during Shear-induced Flocculation," *J. Colloid Interf. Sci.*, **184**, 112 (1996b).
Stover, J. C., *Optical Scattering, Measurement and Analysis*, McGraw-Hill, New York (1990).
Tambo, N., and Y. Watanabe, "Physical Aspect of Flocculation Process I. Fundamental Treasite," *Water Res.*, **13**, 429 (1979).
Tanaka, T., R. Kamimura, R. Fujiwara, and K. Nakanishi, "Cross-flow Filtration of Yeast Broth Cultivated in Molasses," *Biotechnol. Bioeng.*, **43**, 1094 (1994).
Vigil, R. D., and R. M. Ziff, "On the Stability of Coagulation-fragmentation Population Balances," *J. Colloid Interf. Sci.*, **133**, 257 (1989).
Wickramasinghe, S. R., "Washing Cryopreserved Blood Products using Hollow Fibres," *Trans. IChemE*, **77** (Part C), 287 (1999).
Wickramasinghe, S. R., Y. Wu, and B. Han, "Enhanced Microfiltration of Yeast by Flocculation," *Desalination*, **147**, 25 (2002).
Zeitlin, M. A., and L. L. Tavlarides, "On Fluid-fluid Interactions and Hydrodynamics in Dispersed Phase CSTR's: Prediction of Local Concentrations, Transfer Rates and Reaction Conversion," *Int. Symp. on Chemical Reaction Eng.*, Amsterdam, Netherlands (1972).
Zydney, A. L., P. Aimar, M. Meireles, J. M. Pimbley, and G. Belfort, "Use of the Log-normal Probability Density Function to Analyze Membrane Pore-size Distributions—Functional Forms and Discrepancies," *J. Memb. Sci.*, **91**, 293 (1994).

*Manuscript received Sept. 3, 2002, and revision received Jan. 29, 2003.*